Energy Efficient Optimization for Wireless Virtualized Small Cell Networks With Large-Scale Multiple Antenna

Zheng Chang, *Member, IEEE*, Zhu Han, *Fellow, IEEE*, and Tapani Ristaniemi, *Senior Member, IEEE*

***Abstract*— Wireless network virtualization is envisioned as a promising framework to provide efficient and customized services for next-generation wireless networks. In wireless virtualized networks (WVNs), limited radio resources are shared among different services providers for providing services to different users with heterogeneous demands. In this paper, we propose a resource allocation scheme for an orthogonal frequency division multiplexing-based WVN, where one small cell base station equipped with a large number of antennas serves the users with different service requirements. In particular, with the objective to obtain the energy efficiency in the uplink, a joint power, subcarrier, and antenna allocation problem is presented considering availability of both perfect and imperfect channel state information. Subsequently, relaxation and variable transformation are applied to develop the efficient algorithm to solve the formulated non-convex and combinational optimization problem. Extensive simulation studies demonstrate the advantages of our presented system architecture and proposed schemes.**

***Index Terms*— Wireless network virtualization, resource allocation, large scale multiple antenna system, energy efficiency, small cell.**

I. Introduction

THE AIM of 5G is to provide ubiquitous connectivity for any kind of devices and any kind of applications that may benefit from being connected, which may require 1000-fold more capacity, extreme low-latency (under 1 ms), and low energy consumption (90% reduction) for trillions of devices [1]. To realize the vision of essentially unlimited access to information and sharing of data anywhere and anytime for anyone and anything, the recent emerging mobile platforms, such as Software Defined Network (SDN) and Network Function Virtualization (NFV), bring us novel views on the current cellular wireless networks, which urge to rethink the current network infrastructure. The recent advances also open the way to expand SDN/NFV concepts to Radio Access Networks (RANs), creating thus the Wireless Virtualized Networks (WVNs) framework where the execution of RAN functions is moved from dedicated telecom hardware to commoditized IT platforms owned by multiple Infrastructure Providers (InPs). In the context of WVN, both infrastructure and radio resources can be abstracted, sliced and shared [2], and a mobile network operator can rent the radio resources in a virtualized manner. Consequently, the overall expenses of wireless network deployment and operation can be significantly reduced as well [3]. In short, WVN can be considered as the technology in which physical wireless network infrastructure and physical radio resources are abstracted and sliced into virtual wireless resources, and shared by multiple parties with a certain degree of isolation between them.

Although the WVN has the envisioned potential to improve the utilization of wireless resource for the future 5G networks, how to operate it in an efficient manner is still under investigation. Moreover, how to successfully merge or combine the other recent advances with the WVN requires dedicated efforts. With wireless virtualization, the wireless network infrastructure can be decoupled for different services providers, from the services that they provides. Hence, differentiated services can coexist on the same physical infrastructure and their utilities can be maximized accordingly. After the physical resources are abstracted and virtualized, they can be divided into multiple virtual slices and then allocate to different operators or virtual networks. By virtualizing the uplink and downlink resources into slices, the network can operate in a dynamic and reconfigurable manner to fulfill the diverse requirements of the users in different slices.

Meanwhile, on the way towards the gigabytes transmission, it can be expected that the number of antennas at the Base Station (BS) becomes relative large. The resulted large scale multiple antenna system or so call massive Multi-input Multi-output (MIMO) system, will consist of hundreds of deployed antennas at the BS [1]. The increase of number of antennas at the BS can inevitably bring capacity gain to the system in order to provide high speed service rates to a large number of users. On the other hand, the large scale multiple antenna system also faces many challenges, of which the Energy Efficiency (EE) issues emerges as a significant one [4]. As the number of antennas goes large, the relevant energy consumption also increments if all the antennas are active all the time. Thus, how to efficiently operate the BS with a large number of antennas

Manuscript received April 12, 2016; revised September 9, 2016 and December 18, 2016; accepted February 2, 2017. Date of publication February 8, 2017; date of current version April 14, 2017. This work is partially funded by Academy of Finland (Decision 284748) and US NSF CPS-1646607, ECCS-1547201, CCF-1456921, CNS-1443917, ECCS-1405121. The associate editor coordinating the review of this paper and approving it for publication was Z. Zhang.

Z. Chang and T. Ristaniemi are the with the Department of Mathematical Information Technology, University of Jyväskylä, FIN-40014 Jyväkylä, Finland (e-mail: zheng.chang@jyu.fi; tapani.ristaniemi@jyu.fi).

Z. Han is with the Electrical and Computer Engineering Department, University of Houston, Houston, TX 77004 USA (e-mail: zhan2@uh.edu).

Color versions of one or more of the figures in this paper are available online at http://ieeexplore.ieee.org.

Digital Object Identifier 10.1109/TCOMM.2017.2666182

to reduce the energy cost while maintaining the quality of high speed services induces a careful design from the EE point of view.

The investigations on wireless networks virtualization have attracted many interests recently. Liang and Yu [3], [5] provide the overview on the general framework for wireless virtualization and propose a virtual resource allocation scheme for virtualized networks, respectively. A wireless resource slicing scheme has been presented in [6], which can flexibly partition fragmented frequency spectrum into different slices that share the RF front end and antenna. By such, it is shown that the proposed idea can provide a general and clean abstraction to exploit fragmented spectrum in dense deployed WiFi networks. Kamel *et al.* [8] propose a virtualization framework for LTE systems, where the eNB and physical resources are allocated to the service providers by a central entity called hypervior. It can be found that there are several main challenges that WNV faces, including capacity limitation, complete isolation among different coexisted services and signaling overhead [9]. Tseliou *et al.* [9] take into account these challenges and propose a solution for the multiple operator networks where baseband modules of distributed BSs cooperate to reallocate radio resources based on the traffic dynamics. Moreover, insightful discussion on the additional signaling overhead is presented. In [10], the performances of different mobile network sharing schemes, ranging from simple approaches in traditional networks to complex methods that require virtualized infrastructure, are investigated. Utilizing the game theoretic approaches, the authors present a stochastic game framework in [11] to model the interactions between service providers and InPs. Zhu and Zhang present different power and spectrum allocation schemes for the WVN by using game theory. Considering a Cloud-RAN based small cell network with wireless virtualization, Zhang *et al.* [13] present an user-cell association scheme to achieve the target of energy saving and interference limitation. Ibrahim *et al.* [14] present a tractable analytical model for virtualized downlink cellular networks using tools from stochastic geometry. In [15], the virtual resource allocation problem in virtualized small cell networks with full-duplex self-backhaul has been studied.

At the same time, EE in a multiple antenna system has received increasing attentions as well [17]–[19]. Reference [17] has studied the mutual information quantity optimization problem of the MIMO system, showing that increasing number of used antenna leads to the spectrum efficiency increment. As a matter of fact, although the use of MIMO can improve the system spectrum efficiency, the use of a large number of antennas brings significant problem to the EE design. Therefore, for the massive MIMO system, the number of selected antennas should be decided in an optimized manner. The authors focus the performance of transmitting and receiving antenna selection when estimation error exists [18]. In [19], two antenna selection algorithms are presented. Jumba *et al.* [20] combine the concept of massive MIMO and WVN, and then present resource allocation scheme to maximize the throughput performance for such an advanced framework.

As we can see, the small cell network with massive MIMO emerges as as one of the key components of next-generation cellular networks to improve spectrum efficiency. Despite the potential vision of small cell networks with massive MIMO, many research challenges still need to be addressed. One of the main research challenges is resource allocation, which plays a significant role in traditional wireless networks. As WNV directs a potential route towards efficient resource allocation operation by resources abstraction and virtualization, it can offer us a novel view on managing massive antennas in a small cell networks. By such, the resource can be divided into multiple virtual slices and then allocate to different operators so that a dynamic and reconfigurable operation can be achieved to fulfill the diverse requirements of the users in different slices. In this work, our goal is to investigate the problem of resource allocation for achieving uplink EE considering small cell network virtualization. Compared to the aforementioned works, our contributions can be summarized as follows,

- We present the WVN architecture, where a small cell BS (SBS) with a large number of antennas serves a number of users via resource slicing. In the proposed virtualized networks, a joint resource allocation optimization problem for uplink transmission containing power, subcarrier and antenna allocation is formulated with the objective to maximize the EE while maintaining the service quality of each slice.
- To solve formulated mixed combinatorial and non-convex optimization problem, we apply the nonlinear fractional programming method and transfer the original problem into a subtractive form. Then the constraints of the transformed form can be further relaxed and addressed in the dual domain. In addition to the consideration of perfect knowledge of Channel State Information (CSI), we also take the practical issue that imperfect CSI knowledge is available into account into consideration when executing resource allocation decision. By such, the robustness of the proposed scheme can be enhanced.
- The effectiveness of the proposed scheme is demonstrated through extensive simulations. It is shown that by utilizing the WVN in the small cell networks with the proposed virtual resource allocation algorithm, superior performance can be obtained.

The rest of this paper is organized as follows. Section II describes the system model and assumptions. We present the problem formulation in Section III and propose a resource allocation algorithm in Section IV. The performance evaluation is illustrated in Section V through simulation study, and we finally conclude this work in Section VI.

II. System Model

A. Wireless Virtualized Networks

Virtualization has recently moved from traditional server virtualization to wireless virtualization. In stead of virtualizing the computing resources in server virtualization, in the WNV technologies, physical wireless network infrastructure and radio resources can be abstracted and sliced into virtual wireless network resources holding certain corresponding

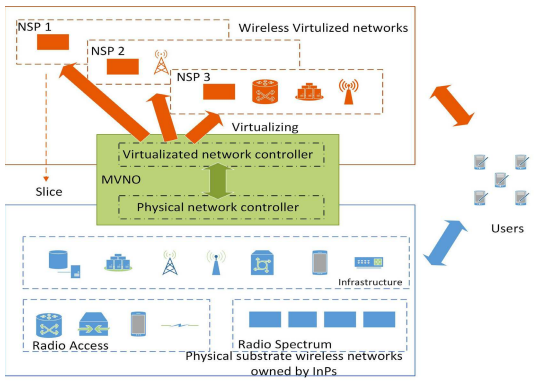

Fig. 1. Wireless Network Virtualization

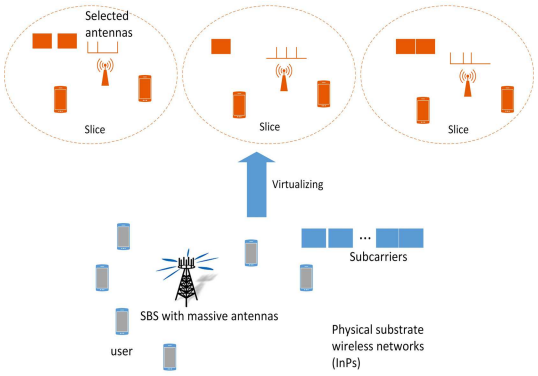

Fig. 2. System Model

functionalities, and shared by multiple parties through isolating each other [9]. Therefore, the physical resources of the InPs need to be abstracted to isolated virtual resources. Then, the virtual resources can be offered to different Network Service Providers (NSPs), who concentrate on providing services to the users. In Fig. 1, a simple illustration of wireless virtualization is presented. Following the general frameworks of WVN [3], [7], [9], in order to offer service to the users, the NSPs in Fig. 1 will ask the InPs about the radio resources. Then, the physical resources, including spectrum, and infrastructures from different InPs will be handled by the physical network controller. The resources can then be abstracted, virtualized and sliced to different virtual resources and provided to different NSPs according to their demands. The virtualization is done by the Mobile Virtual Network Operator (MVNO), of which the rule is to lease and virtualize the physical networks into virtual network based on the requests of NSPs. End users logically connect to the virtual network through which they subscribe to the service, while they physically connect to the cellular network.

In order for the NSPs to provide services to the end-users, attracted and virtualized resources are provided to different NSPs in terms of resource slices. Each resource slice contains a certain amount of radio resources, such as power, frequency spectrum, antennas and related hardware in Fig. 1. The amount of resources that can be allocated to one slice should be based on the Quality of Service (QoS) requirements of the service it needs to provide and the total system utility. To maximize the total utility of all MVNOs, the resource allocation schemes for WVN should be developed to dynamically allocate the virtual resources from the physical substrate wireless networks and then provide services to different users.

The whole virtualization process can be realized in the following way. First, virtual slices can be used to model the virtual resources, similar to the physical resource block in LTE. However, the details of the slices, such as time and frequency, can be negotiated by the MVNO and NSP. For slicing, the MVNO generates a certain number of resource slices for the NSPs based on current network status. Then, the MVNO defines the properties (e.g., virtualized resources) for each slices based on the agreements with NSPs and delivers slices to the corresponding NSPs. After that, each NSP allocates appropriate number of resources to each subscriber based on its QoS (e.g., energy efficiency or delay) and data rate demand, and the MVNO receives such scheduling information about the next potential served users from NSPs. The isolation is done in the way that the MVNO converts the properties of each resource slice to data rate requirements or physical resource requirements and prepares the corresponding physical resources for each user. Finally, the MVNO or the InP allocates physical resources (e.g., BS, radio resource) to each end user based on the current network status.

B. System Assumption

An example of our considered system model is presented in Fig. 2. The physical networks including the hardware (e.g., antennas, etc.), frequency spectrum and other types of radio resources, which are essential for offering wireless access services and are provided by the InPs. Based on the aforementioned virtualization process, the MVNO is able to create different resource slice containing selected antennas and spectrum. In our considered system, the physical network is Orthogonal Frequency Division Multiplexing (OFDM)-based, and it contains a Small cell Base Station (SBS) with $M \gg 1$ antennas and N subcarriers, which is typical in a mmWave-based small cell. In the considered wireless virtualized network architecture in Fig. 2, we can see that there is a centralized controller located in mobile virtual network operator (MVNO), and it can obtain the feedbacks of each users and carry out the scheduling decision among different service operators. Moreover, from [17], we can observe the number of bits needed for feedback falls off rapidly as the number of antennas increases. Therefore, for the considered system with a large number of antennas, the feedback overhead is considered as sufficiently low. In order to provide the services to the users, the resources will be slicing into S pieces and the set of all slices is denoted as $\mathcal{S}$. Each slice $s \in \mathcal{S}$ has a set of users with single antenna denoted as $\mathcal{U}_s$. The number of users in each slice is $U_s = |\mathcal{U}_s|$. As for each slice, the provided services are varied and the QoS requirements are different. Thus, we consider there is a minimum data rate or QoS requirement r_s^{rsv} for each slice. Then, the total number of $U = \sum_{s\in\mathcal{S}} U_s$ and we assume that $M \gg U$, which is practical for the small cell networks with a large scale of multiple antennas. We consider that for each slice, a set of

subcarriers is allocated, and we denote $\boldsymbol{\omega} \in \mathbb{C}^{U\times N}$ as the subcarrier-slice assignment indicator matrix, where each row vector $\boldsymbol{\omega}_{u_s} = [\omega_{u_s,1}, \omega_{u_s,2}, ..., \omega_{u_s,n}, ..., \omega_{u_s,N}]$, and we have

$$\omega_{u_s,n} = \begin{cases} 1, & \text{if subcarrier } n \text{ is allocated to the user } u_s; \\ 0, & \text{otherwise.} \end{cases} \quad (1)$$

Further, we also define an antenna allocation matrix $\boldsymbol{\alpha} \in \mathbb{C}^{U\times N}$, in which $\alpha_{u_s,n}$ is the number of antennas allocated to the user u_s in slice s on subcarrier n and for each slice s. Meanwhile, the number of allocated antennas for each slice should be controlled to preserve the fairness between slices and to improve the energy efficiency [4]. Thus, we define a set of reserved antenna for each slice as $\{\alpha_s^{min}, ..., \alpha_s^{max}\}$. Note that the set of reserved antenna is a discrete set and the selected antenna is also a integer. Later we will show how to transfer it to the continous counterpart and address the antenna selection problem accordingly.

III. Problem Formulation

In this section, we present the problem formulation. In particular, we consider the resource allocation in the uplink (UL) and formulate a joint optimization of subcarrier, power and antenna for each slice in the virtualized small cell networks.

A. Channel Model

Let $h_{u_s,n,\beta_{u_s,n}}$ be the channel coefficient of user u_s in slice s on subcarrier n and antenna $\beta_{u_s,n}$. Then, for the allocated $\alpha_{u_s,n}$ antennas, we have the corresponding channel coefficient $\boldsymbol{h}_{u_s,n} \in \mathcal{C}^{1\times\alpha_{u_s,n}}$, which is modeled as independent identically distributed (i.i.d.) complex Gaussian random variables with zero mean and unit variance .[1] We denote d_{u_s} as the path loss factor from the SBS to user u_s. We also denote that $P_{u_s,n}$ as the transmit power from the user u_s to the BS in slice s on subcarrier n.

When considering the imperfect knowledge of CSI, we denote $\hat{h}_{u_s,n,m}$ as the estimated channel coefficient on antenna m, which can be expressed

$$\hat{h}_{u_s,n,m} = h_{u_s,n,m} + z_{u_s,n,m}, \quad (2)$$

where $z_{u_s,n,m}$ is the channel estimation error and we assume that $z_{u_s,n,m} \sim \mathcal{N}(0, \sigma_z^2)$.

Accordingly, in the perfect CSI case, the received signal on UL at the BS after from user u_s on subcarrier n is

$$y_{u_s,n} = \sqrt{P_{u_s,n} d_{u_s}} \boldsymbol{b}_{u_s,n} \boldsymbol{h}_{u_s,n} \boldsymbol{x}_{u_s,n} + \boldsymbol{e}_{u_s,n}, \quad (3)$$

where $\boldsymbol{x}_{u_s,n}$ is the transmitted signal and $\boldsymbol{e}_{u_s,n}$ is the channel n noise. $\boldsymbol{b}_{u_s,n}$ is the precoding vector and the maximum ratio transmission design is applied, i.e., $\boldsymbol{b}_{u_s,n} = \frac{\boldsymbol{h}_{u_s,n}}{\|\boldsymbol{h}_{u_s,n}\|}$. $\boldsymbol{e}_{u_s,n}$ is the additive Gaussian noise and follows $\mathcal{N}(0, \sigma^2)$. Similarly, considering the imperfect CSI case, we have the received signal as

$$\hat{y}_{u_s,n} = \sqrt{P_{u_s,n} d_{u_s}} \boldsymbol{b}_{u_s,n}^{im} \hat{\boldsymbol{h}}_{u_s,n} \boldsymbol{x}_{u_s,n} + \boldsymbol{e}_{u_s,n}. \quad (4)$$

where $\boldsymbol{b}_{u_s,n}^{im}$ is the precoding vector. In a massive MIMO system, with the increase of the number of antennas, the channel hardening effect emerges [16], [17]. In other words, the mutual information fluctuation decreases rapidly relative to its mean. Therefore, in order to obtain the expected data rate of the considered system with imperfect CSI, we first study the mutual information distributions with/without antenna selection. To this end, based on the above definitions, we can obtain the mutual information distribution of the users u_s without antenna selection as follows [17],

$$I_{MI} \sim \mathcal{N}\left(log_2(1 + M\gamma_{u_s,n}), \frac{(log_2 e)^2}{M}\right), \quad (5)$$

where $\mathcal{N}$ represents standard normal distribution and $\gamma_{u_s,n} = d_{u_s} P_{u_s,n}/\sigma^2$ is the SNR and σ^2 is the channel noise variance. Moreover, when considering imperfect CSI, the mutual information distribution of the users u_s without antenna selection can be

$$I_{MI}^{im} \sim \mathcal{N}\left(\log_2\left(1 + M\rho_{u_s,n}\right), \frac{(\log_2 e)^2}{M}\right), \quad (6)$$

where $\rho_{u_s,n}$ represents the SNR with the imperfect CSI and channel noise on subcarrier n in slice s, i.e., $\rho_{u_s,n} = \frac{d_{u_s} P_{u_s,n}}{\sigma^2 + d_{u_s} P_{u_s,n} \sigma_z^2}$. The derivation of (6) is given in Appendix A.

As the number of antennas grows, the channel quickly "hardens", in the sense that the mutual information fluctuation decreases rapidly relative to its mean. This form of channel hardening is generally welcome for voice and other traffic that is sensitive to channel fluctuations and delay. In [17], the implementation, scheduling and rate feedback of the channel hardening result are discussed. It can be found that the number of bits needed for rate feedback and the outage probability decreases as the number of receive antennas increases. Therefore, we aim to find if there is a similar channel hardening phenomenon in the considered antenna selection system. Then, similar to the analysis in (5) and (6), mutual information distributions of users u_s with antenna selection when considering perfect CSI and imperfect CSI are presented in **Lemma 1** and **Lemma 2**, respectively.

Lemma 1: When assuming full CSI is known, for a large M and selected antenna $\alpha_{u_s,n}$, an approximation of the distribution of the mutual information of user u_s on subcarrier n is given as follows,

$$I_{u_s,n} \sim \mathcal{FN}\left(log_2\left(1 + \left(1 + \ln\frac{M}{\alpha_{u_s,n}}\right)\gamma_{u_s,n}\alpha_{u_s,n}\right), \frac{(log_2 e)^2 \gamma_{u_s,n}^2 \alpha_{u_s,n}(2 - \frac{\alpha_{u_s,n}}{M})}{\left(1 + \left(1 + \ln\frac{M}{\alpha_{u_s,n}}\right)\gamma_{u_s,n}\alpha_{u_s,n}\right)^2}\right), \quad (7)$$

where $\mathcal{FN}$ represents the folded normal distribution.

Proof: The proof of **Lemma 1** is shown in Appendix B. ∎

[1] We consider this work can be applied to the case where CSI information can be obtained or known. For the mobility case of which the CSI can not be perfectly obtained, we consider our problem can be addressed by restricting the outage probability. In fact, in such a case, there are several ways for the BS/operator to obtain the knowledge of the (at least approximated) location of the mobility user, e.g., via GPS or location updates in cellular network. Based on such information, the path loss and slow fading effect can be approximated. Although the fast fading effect cannot be perfectly known, the problem can be addressed by putting a constraint on the outage probability.

Obviously, if $\alpha_{u_s,n} = M$ (M is sufficiently large), the expected value of the distribution expression is as the same as the one in (5), and the variance is approximately the same. From **Lemma 1** and its proof, we can see that it is not necessary to obtain the channel gain of each antenna. Rather, the approximation of mutual information depends on the number of antennas at BS, the selected number of antennas and transmit SNR. Therefore, adding antenna selection does not affect the channel's hardening. Then we can also derive the mutual information when considering the imperfect CSI.

Lemma 2: In the considered system, a numerically approximation of the mutual information $I^{im}_{u_s,n}$ considering imperfect CSI is as follows:

$$I^{im}_{u_s,n} \sim \mathcal{FN}\Big(\log_2\left(1+\left(1+\ln\frac{M}{\alpha_{u_s,n}}\right)\rho_{u_s,n}\alpha_{u_s,n}\right), \frac{(\log_2 e)^2\rho^2_{u_s,n}\alpha_{u_s,n}(2-\frac{\alpha_{u_s,n}}{M})}{(1+(1+\ln\frac{M}{\alpha_{u_s,n}})\rho_{u_s,n}\alpha_{u_s,n})^2}\Big). \quad (8)$$

Proof: The proof of **Lemma 2** is similar to the one of **Lemma 1** and we omit here. ∎

According to the mutual information distribution, we can obtain the expected data rate of the user u_s in the following theorem.

Theorem 1: The expected data rate of the user u_s with or without perfect CSI can be given as

$$R_{u_s,n} = \begin{cases} \log_2\left(1+\left(1+\ln\frac{M}{\alpha_{u_s,n}}\right)\gamma_{u_s,n}\alpha_{u_s,n}\right), \\ \textit{if perfect CSI;} \\ \log_2\left(1+\left(1+\ln\frac{M}{\alpha_{u_s,n}}\right)\rho_{u_s,n}\alpha_{u_s,n}\right), \\ \textit{if imperfect CSI.} \end{cases} \quad (9)$$

Proof: The proof can be simply derived from **Lemma 1** and **Lemma 2**. ∎

To this end, by denoting $\mathcal{N}_C$ as the set of all the subcarriers, we can formulate the expected data rate of all the slices in $\mathcal{S}$ as follows,

$$\mathcal{C}(\boldsymbol{P},\boldsymbol{\alpha},\boldsymbol{\omega}) = \sum_{s\in\mathcal{S}}\sum_{u_s\in\mathcal{U}_s}\sum_{n\in\mathcal{N}_C}\omega_{u_s,n}R_{u_s,n}. \quad (10)$$

B. Energy Consumption Model

In this work, we use the power consumption model in [26] and [28], of which the total power consumption consists of the transmit power and the circuit power consumption. Here, we use P_c to represent the constant circuit power consumption per antenna chain which includes the power dissipations in the converters, filter, mixer, and frequency synthesizer which is independent of the actual transmitted power. We also denote κ as power amplifier efficiency parameter and P_0 as the basic operating power consumed at the BS independent of the number of transmit antennas, e.g., baseband power consumption. Correspondingly, the total power consumption of all the slices can be expressed as

$$\Upsilon(\boldsymbol{P},\boldsymbol{\alpha},\boldsymbol{\omega}) = \sum_{s\in\mathcal{S}}\sum_{u_s\in\mathcal{U}_s}\sum_{n\in\mathcal{N}_C}\omega_{u_s,n}\kappa P_{u_s,n} + P_0 + \max_{u_s,n}\{\omega_{u_s,n}\alpha_{u_s,n}\}P_c. \quad (11)$$

Note that the physical meaning of the term $\max_{s,u_s}\{\omega_{u_s,n}\alpha_{u_s,n}\}$ is that an antenna is activated and consumes power even it is used only by some of the users. Therefore, several users can share same antenna at the BS.

C. Energy Efficiency Objective

Based on the above analysis, we are able to formulate the **Problem 1**, of the which the objective is to maximize EE of the considered system.

$$\mathbf{P1}: \max_{\boldsymbol{P},\boldsymbol{\alpha},\boldsymbol{\omega}} \mathcal{E}(\boldsymbol{P},\boldsymbol{\alpha},\boldsymbol{\omega}) = \frac{\mathcal{C}(\boldsymbol{P},\boldsymbol{\alpha},\boldsymbol{\omega})}{\Upsilon(\boldsymbol{P},\boldsymbol{\alpha},\boldsymbol{\omega})}, \quad (12)$$

s.t.

$$\begin{aligned} C1: &\sum_{s\in\mathcal{S}}\sum_{u_s\in\mathcal{U}_s}\omega_{u_s,n}\le 1, \omega_{u_s,n}\in\{0,1\}, \\ C2: &\sum_{u_s\in\mathcal{U}_s}\sum_{n\in\mathcal{N}_C}\omega_{u_s,n}R_{u_s,n} > r_s^{rsv}, \\ C3: &\sum_{n\in\mathcal{N}_C}\omega_{u_s,n}P_{u_s,n}\le P_{u_s}^{max}, \\ C4: &\sum_{u_s\in\mathcal{U}_s}\sum_{n\in\mathcal{N}_C}\omega_{u_s,n}\alpha_{u_s,n}\in\{\alpha_s^{min},\ldots,\alpha_s^{max}\}. \end{aligned} \quad (13)$$

The formulated objective in (12) is under the constraints in (13). In (13), **C1** is to ensure the exclusive sub-carrier allocation; **C2** is able to guarantee the minimum required rate for each slice; **C3** puts the constraint on the transmit power limitation for each user. In **C4**, α_s^{min} and α_s^{max} are the minimum number of reserved antennas and the maximum allowable number of allocated antennas for slice s, respectively.

As one can observe, **P1** has a non-convex structure with combinatorial properties and finding the optimal solution of **P1** involves high computational complexity. Next, we propose an efficient algorithm to solve this problem by applying the nonlinear fractional programming technique, variable transformations and constraint relaxation.

IV. Energy Efficient Resource Allocation

A. Problem Transformation

The fractional objective function in (12) can be classified as a nonlinear fractional program [22]. For the sake of notational simplicity, $\mathcal{F}$ is defined as the set of feasible solutions of the optimization problem **P1**. Without loss of generality, for $\forall\{\boldsymbol{P},\boldsymbol{\alpha},\boldsymbol{\omega}\}\in\mathcal{F}$ we define the maximum EE q^* as

$$q^* = \mathcal{E}(\boldsymbol{P}^*,\boldsymbol{\alpha}^*,\boldsymbol{\omega}^*) = \max_{\boldsymbol{P},\boldsymbol{\alpha},\boldsymbol{\omega}}\frac{\mathcal{C}(\boldsymbol{P},\boldsymbol{\alpha},\boldsymbol{\omega})}{\Upsilon(\boldsymbol{P},\boldsymbol{\alpha},\boldsymbol{\omega})}, \quad (14)$$

where $\boldsymbol{P}^*,\boldsymbol{\alpha}^*,\boldsymbol{\omega}^*$ are the optimal solutions for $\boldsymbol{P},\boldsymbol{\alpha},\boldsymbol{\omega}$, respectively. We can introduce the following Theorem on the optimal q^*.

Theorem 2: q can reach its optimal value q^* if and only if

$$\boldsymbol{P2}: \max_{\boldsymbol{P},\boldsymbol{\alpha},\boldsymbol{\omega}}\mathcal{C}(\boldsymbol{P},\boldsymbol{\alpha},\boldsymbol{\omega}) - q\Upsilon(\boldsymbol{P},\boldsymbol{\alpha},\boldsymbol{\omega}) = 0. \quad (15)$$

Proof: The proof is derived from [22]. ∎

Theorem 2 reveals that for an optimization problem with an objective function in fractional form, e.g. (12), there is an

Algorithm 1 Iterative Algorithm for Obtaining q^*

1: Set maximum tolerance δ;
2: **while** (not convergence) **do**
3: Solve the problem (16) for a given q and obtain antenna, power and subcarrier allocation $\{\boldsymbol{P}', \boldsymbol{\alpha}', \boldsymbol{\omega}'\}$;
4: **if** $\mathcal{C}(\boldsymbol{P}', \boldsymbol{\alpha}', \boldsymbol{\omega}') - q\Upsilon(\boldsymbol{P}', \boldsymbol{\alpha}', \boldsymbol{\omega}') \leq \delta$ **then**
5: Convergence = true;
6: **return** $\{\boldsymbol{P}^*, \boldsymbol{\alpha}^*, \boldsymbol{\omega}^*\} = \{\boldsymbol{P}', \boldsymbol{\alpha}', \boldsymbol{\omega}'\}$ and obtain q^* by (14);
7: **else**
8: Convergence = false;
9: **return** Obtain $q = \frac{\mathcal{C}(\boldsymbol{P}', \boldsymbol{\alpha}', \boldsymbol{\omega}')}{\Upsilon(\boldsymbol{P}', \boldsymbol{\alpha}', \boldsymbol{\omega}')}$;
10: **end if**
11: **end while**

equivalent objective function in a subtractive form. As a result, we are able to focus on the equivalent objective function and find the solution. In order to obtain q^*, an iterative algorithm with guaranteed convergence [22] can be applied and it can be found in Algorithm 1. In Algorithm 1, obtaining the optimal solution of power, subcarrier, and antenna allocation involves finding the optimal value of q in (14). For given q, we are able to reach a solution of power, subcarrier, and antenna allocation. As we can see from **Theorem 2**, for a given solution of $\{\boldsymbol{P}, \boldsymbol{\alpha}, \boldsymbol{\omega}\}$, we can find the solution of q by 16. Then iterative method is applied to optimal solution of $\{\boldsymbol{P}, \boldsymbol{\alpha}, \boldsymbol{\omega}\}$ and q.

During the iteration, in order to achieve q^*, we need to address the following problem (**P2**) with q:

$$\max_{\boldsymbol{P}, \boldsymbol{\alpha}, \boldsymbol{\omega}} \mathcal{C}(\boldsymbol{P}, \boldsymbol{\alpha}, \boldsymbol{\omega}) - q\Upsilon(\boldsymbol{P}, \boldsymbol{\alpha}, \boldsymbol{\omega}), \tag{16}$$

s.t.

$$C1 - C3. \tag{17}$$

To this end, we can address the fractional programming problem in a subtractive form. However, it can also be found that (**P2**) is still a non-convex problem due to the integer programming involved. Tackling the mixed convex and combinatorial optimization problem requires a prohibitively high complexity. Another solution which can balance the computational complexity and optimality can be obtained when addressing such a problem in the dual domain. For the formulated optimization problem, as the convexity does not hold (e.g., mixed integer programming), addressing it in dual domain may result in a duality gap between primal and dual problem. As discussed and proved in [21] and [23], in the considered multi-carrier systems, the duality gap of such a non-convex resource allocation problem satisfying the time-sharing condition is negligible as the number of subcarriers becomes sufficiently large e.g., 64. To address the problem, we relax $\omega_{u_s,n}$ to be a real variable in the range of $[0, 1]$ instead of a Boolean. Then, $\omega_{u_s,n}$ can be interpreted as a time sharing factor for utilizing subcarriers. As one can see, the optimization problem obviously is able to satisfy the time-sharing condition, it can be solved by using the dual method and the solution is asymptotically optimal [23], [24].

B. Proposed Solution

Based on above analysis, we can define two new variables, $\phi_{u_s,n}$ and $\varphi_{u_s,n}$ as follows,

$$\begin{aligned} \phi_{u_s,n} &= \omega_{u_s,n} P_{u_s,n}, \\ \varphi_{u_s,n} &= \omega_{u_s,n} \alpha_{u_s,n}. \end{aligned} \tag{18}$$

Now, instead of finding the solution of $\alpha_{u_s,n}$, we can address $\varphi_{u_s,n}$ to solve the problem of antenna selection. Then, **P2** can be reformed as

$$\mathbf{P3}: \quad \max_{\boldsymbol{\phi}, \boldsymbol{\varphi}, \boldsymbol{\omega}} \widetilde{\mathcal{C}}(\boldsymbol{\phi}, \boldsymbol{\varphi}, \boldsymbol{\omega}) - q\widetilde{\Upsilon}(\boldsymbol{\phi}, \boldsymbol{\varphi}, \boldsymbol{\omega}), \tag{19}$$

s.t.

$$\begin{aligned} \widetilde{C1}: &\quad \sum_{s \in \mathcal{S}} \sum_{u_s \in \mathcal{U}_s} \omega_{u_s,n} \leq 1, \omega_{u_s,n} \in [0, 1], \\ \widetilde{C2}: &\quad \sum_{u_s \in \mathcal{U}_s} \widetilde{R}_{u_s} > r_s^{rsv}, \\ \widetilde{C3}: &\quad \sum_{n \in \mathcal{N}_C} \phi_{u_s,n} \leq P_{u_s}^{max}. \\ \widetilde{C4}: &\quad \alpha_s^{min} \leq \sum_{u_s \in \mathcal{U}_s} \sum_{n \in \mathcal{N}_C} \varphi_{u_s,n} \leq \alpha_s^{max}. \end{aligned} \tag{20}$$

In (19), $\boldsymbol{\phi}$ and $\boldsymbol{\varphi}$ are the vectors of $\phi_{u_s,n}$ and $\varphi_{u_s,n}$, respectively. According to (10) and (18), $\widetilde{\mathcal{C}}(\boldsymbol{\phi}, \boldsymbol{\varphi}, \boldsymbol{\omega})$ is given as

$$\widetilde{\mathcal{C}}(\boldsymbol{\phi}, \boldsymbol{\varphi}, \boldsymbol{\omega}) = \sum_{s \in \mathcal{S}} \sum_{u_s \in \mathcal{U}_s} \sum_{n \in \mathcal{N}} \omega_{u_s,n} \widetilde{R}_{u_s,n}, \tag{21}$$

where $\widetilde{R}_{u_s,n}$ can be expressed as

$$\widetilde{R}_{u_s,n} = \begin{cases} \log_2\left(1 + \left(1 + \ln \frac{M\omega_{u_s,n}}{\varphi_{u_s,n}}\right) \gamma_{u_s,n} \frac{\varphi_{u_s,n}}{\omega_{u_s,n}}\right), \\ \text{if perfect CSI;} \\ \log_2\left(1 + \left(1 + \ln \frac{M\omega_{u_s,n}}{\varphi_{u_s,n}}\right) \rho_{u_s,n} \frac{\varphi_{u_s,n}}{\omega_{u_s,n}}\right), \\ \text{if imperfect CSI.} \end{cases} \tag{22}$$

Similarly, $\widetilde{\Upsilon}(\boldsymbol{\phi}, \boldsymbol{\varphi}, \boldsymbol{\omega})$ is

$$\begin{aligned} \widetilde{\Upsilon}(\boldsymbol{P}, \boldsymbol{\alpha}, \boldsymbol{\omega}) = &\sum_{s \in \mathcal{S}} \sum_{u_s \in \mathcal{U}_s} \sum_{n \in \mathcal{N}_C} \kappa \phi_{u_s,n} \\ &+ P_0 + \max_{u_s,n} \varphi_{u_s,n} P_c. \end{aligned} \tag{23}$$

Since **P3** is a convex optimization problem with involves continuous variables and convex objective function, we can solve it in the dual domain. The Lagrange function of **P3** can be given as

$$\begin{aligned} \mathcal{L}(\boldsymbol{\phi}, \boldsymbol{\varphi}, \boldsymbol{\omega}, \boldsymbol{\lambda}, \boldsymbol{\mu}) = &\widetilde{\mathcal{C}}(\boldsymbol{\phi}, \boldsymbol{\varphi}, \boldsymbol{\omega}) - q\widetilde{\Upsilon}(\boldsymbol{\phi}, \boldsymbol{\varphi}, \boldsymbol{\omega}) \\ &- \sum_{u_s \in \mathcal{U}_s} \lambda_{u_s} \left(\sum_{n \in \mathcal{N}} \phi_{u_s,n} - P_{u_s}^{max} \right) \\ &- \sum_{s \in \mathcal{S}} \mu_s \left(r_s^{rsv} - \sum_{u_s \in \mathcal{U}_s} \widetilde{R}_{u_s} \right). \end{aligned} \tag{24}$$

where λ_{u_s} and μ_s are the Lagrange multipliers for ***C2*** and ***C3***, respectively. $\boldsymbol{\lambda}$ and $\boldsymbol{\mu}$ are corresponding vectors for λ_{n_s} and μ_s, respectively. Then the dual function is

$$\min_{\boldsymbol{\lambda}, \boldsymbol{\mu}} \max_{\boldsymbol{\phi}, \boldsymbol{\varphi}, \boldsymbol{\omega}} \mathcal{L}(\boldsymbol{\phi}, \boldsymbol{\varphi}, \boldsymbol{\omega}, \boldsymbol{\lambda}, \boldsymbol{\mu}). \tag{25}$$

By using the Lagrange dual decomposition, the dual problem (25) can be decomposed into two layers, minimization of (24) which is the inner problem and maximization of (25) which is the outer problem. The dual problem can be solved by addressing both problems iteratively, where in each iteration, the optimal antenna selection, power allocation and subchannel allocation can be obtained by using the Karush-Kuhn-Tucker (KKT) conditions for a fixed set of Lagrange multipliers, and the outer problem is solved using the (sub)gradient method [25]. First, by applying the KKT conditions and given allocated subcarrier, we can obtain the power allocation as

$$P_{u_s,n} = \begin{cases} \left[\frac{\alpha_{u_s,n} d_{u_s} \bar{\mu}_s - \bar{\lambda}_{u_s}\sigma^2 \ln 2 + \alpha_{u_s,n} d_{u_s} \bar{\mu}_s \ln \frac{M}{\alpha_{u_s,n}}}{\alpha_{u_s,n} d_{u_s} \bar{\lambda}_{u_s} \ln 2 \left(1+\ln \frac{M}{\alpha_{u_s,n}}\right)}\right]^+, \\ \text{if perfect CSI;} \\ \Omega, \\ \text{otherwise,} \end{cases} \tag{26}$$

where $\bar{\mu}_s = 1 + \mu_s$, $\bar{\lambda}_{u_s} = q\kappa + \lambda_{u_s}$, and Ω is given in (27), as shown at the bottom of this page, where

$$\begin{aligned} \Gamma_1 &= d_{u_s}\sigma^2 \bar{\lambda}_{u_s}\sigma_z^2, \\ \Gamma_2 &= \sigma\sqrt{\alpha_{u_s,n}\bar{\lambda}_{u_s}}, \\ \Gamma_3 &= \alpha_{u_s,n} d_{u_s}\sigma_z^2. \end{aligned} \tag{28}$$

Similarly, the optimal number of antennas $\varphi_{u_s,n}$ can be obtained by addressing the following equation numerically

$$\frac{\bar{\mu}_s \ln \frac{M}{\varphi_{u_s,n}}}{\ln 2 \left(1+\varphi_{u_s,n}\vartheta\right)\left(1+\ln \frac{M}{\varphi_{u_s,n}}\right)} = P_c q. \tag{29}$$

where $\vartheta = \min\{\gamma_{u_s,n}\}$ if perfect CSI is considered, otherwise $\vartheta = \min\{\rho_{u_s,n}\}$. Here, the sub-optimality should be considered for the practical case, i.e., $\alpha_{u_s,n} = \lfloor \varphi_{u_s,n} \rfloor$, which is required for fulfilling the combinatorial constraint. Eventually, (29) reveals that BS will use the same number of antennas for all the users. Such a phenomena makes sense and it can be interpreted by the following example: Suppose user 1 and user 2 are using N_1 and N_2 antennas such that $N_1 \leq N_2$. From the second user perspective, the cost for $N_1 - N_2$ antennas is paid already. Therefore, since no extra cost has to be paid, the second user will use extra antennas until $N_2 = N_1$, which can bring benefit, i.e., throughput, to the system performance. Finally, for the subcarrier allocation, we take the derivative of the subproblem objective function (24) with respective to $\omega_{u_s,n}$ and obtain

$$\begin{aligned} \Pi_{u_s,n} = &\frac{\ln\left(1+\ln\left(1+\vartheta\frac{M}{\alpha_{u_s,n}}\right)\right)}{\ln 2} \\ &-\lambda_{u_s} P_{u_s,n} - q(\kappa P_{u_s,n} + \alpha_{u_s,n} P_c). \end{aligned} \tag{30}$$

In (30), $\Pi_{u_s,n} = 0$ has the physical meaning that user u_s with negative scheduled data rate on subcarrier n is not selected as they can only provide a negative marginal benefit to the system. On the contrary, if a user enjoys good channel conditions with a positive data rate on subcarrier n, it can provide a higher benefit to the whole system. Thus, the allocation of subcarrier n to user u_s is based on the following policy

$$\omega_{u_s,n} = \begin{cases} 1, & \text{if } \Pi_{u_s,n} > 0; \\ 0, & \text{otherwise.} \end{cases} \tag{31}$$

To solve the outer problem and obtain the lagrangian multipliers $\boldsymbol{\lambda}$ and $\boldsymbol{\mu}$, the gradient method can be applied,

$$\begin{aligned} \lambda_{n_s}(l+1) &= [\lambda_{n_s}(l) - \triangle\lambda_{n_s}(P_{u_s}^{max} - \sum_{n\in\mathcal{N}} \phi_{u_s,n})]^+, \\ \mu_s(l+1) &= [\mu_s(l) - \triangle\mu_s(\sum_{u_s\in\mathcal{U}_s} \widetilde{R}_{u_s} - r_s^{rsv})]^+, \end{aligned} \tag{32}$$

where l is iteration index, $[x]^+ = \max\{0, x\}$, $\triangle\lambda_{n_s}$, and $\triangle\mu_s$ are the step sizes.

TABLE I
SIMULATION PARAMETERS

Parameter	Value
Number of antenna M	100
Power consumption per antenna P_c	43 mW
Constant circuit power consumption P_c	50 mW
Number of subcarriers N	64
α_s^{min} and α_s^{max}	10 and 50
Power amplifier efficiency κ	5
Number of users U	5
P_{us}^{max} (unless specified)	23 dBm
Error variance of imperfect CSI (unless specified)	0.1
Noise variance	1

V. SIMULATION RESULTS

In this section, the performance of the proposed scheme is presented and evaluated by simulation. Some key simulation parameters are from [27] and [28], and are given in Table 1.

First, we show the accuracy of our analytic results in (7) and (8). It can be found that with different M and SNR, they all match perfectly. From Fig. 3, we can see that 90% of the mutual information of full antennas can be achieved with only a quarter of the antennas selected. In Fig. 4, we find that

$$\begin{aligned} \Omega = &\frac{-2\Gamma_1 \ln 2 - 2\sigma_z^2\Gamma_1 \ln 2 - 2\sigma_z^2\Gamma_1 \ln(2+\frac{M}{\alpha_{u_s,n}})}{2(d_{u_s}^2\bar{\lambda}_{u_s} + \Gamma_3 d_{u_s}\ln 2 + \Gamma_3 d_{u_s}\ln(2+\frac{M}{\alpha_{u_s,n}}))} \\ &+ \frac{d_{u_s}\sigma_z^2 \ln 2\Gamma_2\sqrt{1+\ln\frac{M}{\alpha_{u_s,n}}}\sqrt{4d_{u_s}\bar{\mu}_s + 4\Gamma_3\bar{\mu}_s + \Gamma_2^2\sigma_z^4\ln 2 + 4\bar{\mu}_s\Gamma_3\ln\frac{M}{\alpha_{u_s,n}} + \Gamma_2^2\sigma_z^4\ln(2+\frac{M}{\alpha_{u_s,n}})}}{2(d_{u_s}^2\bar{\lambda}_{u_s} + \Gamma_3 d_{u_s}\ln 2 + \Gamma_3 d_{u_s}\ln(2+\frac{M}{\alpha_{u_s,n}}))}, \end{aligned} \tag{27}$$

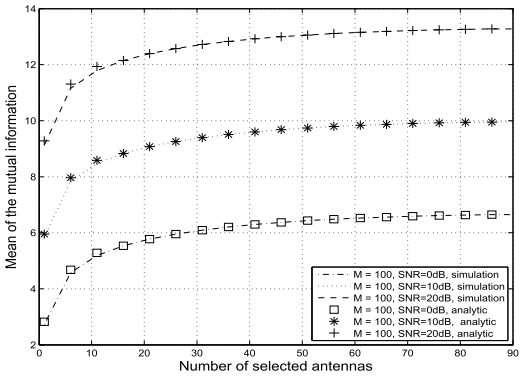

Fig. 3. The effect of the number of selected antennas on the mean of the mutual information.

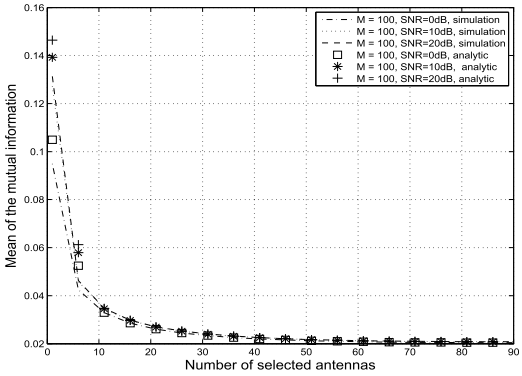

Fig. 4. The effect of the number of selected antennas on the variance of the mutual information.

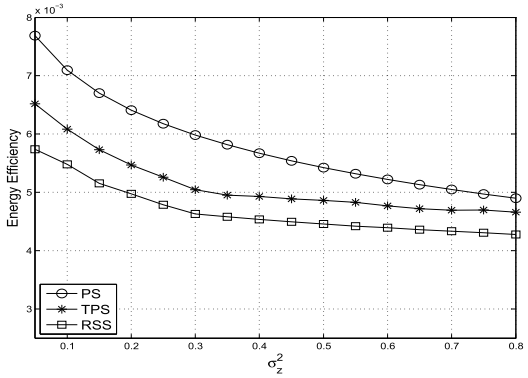

Fig. 5. Comparison of three schemes, EE vs. different variance of imperfect CSI estimation.

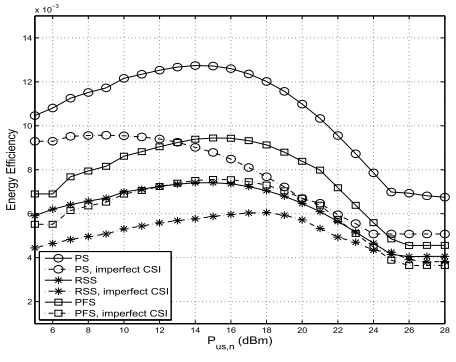

Fig. 6. Comparison of three schemes, EE vs. different transmit power of user.

the variance can be very small with large M. Moreover, for a fixed SNR, when the number of selected antennas is very small, the channel hardens at a lower rate. But for a large range of selected antennas, channel hardens at a high rate almost the same as the case of full antennas. It can be observed that the asymptotic distribution is also very accurate for even small M. These simulations are consistent with our derived result in the lemmas and the relevant discussions.

In addition, we also compare our Proposed Scheme (PS) with the other advanced schemes to show the effectiveness of our proposed scheme. Specifically, we compare our scheme with the one with Random Subcarrier allocation Scheme (RSS), the one with Proportional Fair subcarrier allocation Scheme (PFS), the one with Equal Power allocation Scheme (EPS), a Throughput-based resource allocation Scheme (TPS) [20], and the one without Antenna Selection (nonAS) [29], and Weight Sum resource allocation Scheme (WSS) [30].

We examine the effect of imperfect CSI estimation on the system performance in Fig. 5. In this figure, by varying variance of channel estimation error, i.e., the value of σ_z^2, the impact on EE can be observed. From Fig. 5, we can see that when the increase of estimation error leads to a decrease of system EE. For example, when σ_z^2 is about 0.8, EE is decreased about 25% compared to the one when perfect CSI is assumed. Moreover, we also plot the EE performance when the RSS and TPS are considered instead of the proposed one. We can also observe the same performance degradation due to the CSI imperfection from the results of Random SA. It can be also found that our proposed scheme outperform the TPS and RSS in terms of the EE performance. This is mainly due to the reason that in TPS, throughput is the major concern and more transmit power or antennas are used.

In Fig. 6, we validate the effectiveness of our proposed resource allocation scheme by comparing our proposed scheme with the RSS and PFS. The different values of the EE are obtained by varying the allowed transmit power at the user $P_{us,n}$. In the proposed scheme, we consider the antenna allocation and subcarrier allocation. In the RSS scheme, the proposed antenna selection is used and the subcarriers are randomly assigned to different users and in the PFS, the subcarrier and power is fairly allocated. The EE performance comparison among these three schemes is presented together with the cases that imperfect CSI are assumed. In this figure, we consider $\sigma_z^2 = 0.1$. As we can see, the maximum EE can be obtained when $P_{us,n}$ is about 15dBm when perfect CSI is assumed. When more power is used at the user, it can be the case that higher throughput can be obtained, but the overall EE is degraded due to the cost of energy consumption. Thus, the optimal power allocation scheme is necessary to optimize the EE performance. The results in Fig. 6 confirm the observation in Fig. 5 that the imperfect CSI estimation decreases the system EE. Moreover, it is shown that our proposed subcarrier allocation has a better EE performance

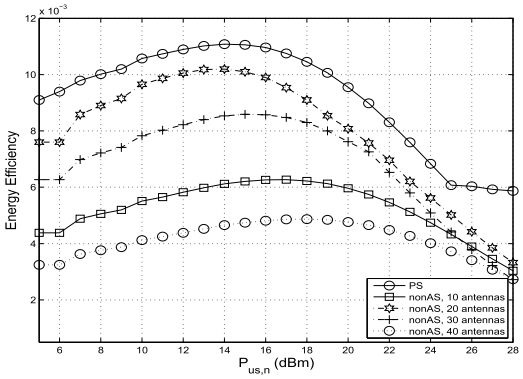

Fig. 7. Impact of antenna selection and transmit power.

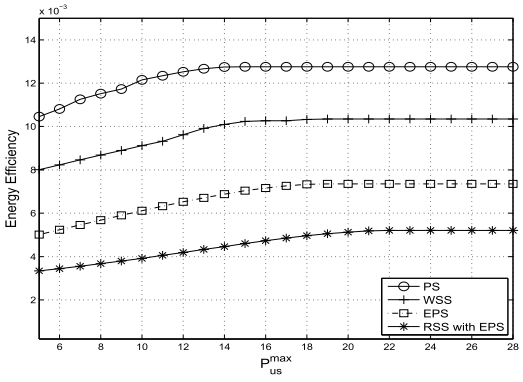

Fig. 8. EE performance comparison of four resource allocation schemes.

over the RSS and PFS, no matter what transmit power is used.

The impact of the number of antennas on the EE performance is presented in Fig. 7, where we alternate the number of used antenna at the BS and plot the corresponding performance comparing with the proposed antenna selection scheme. It can be observed that activating a fixed number of antennas $\alpha_{u_s,n}$ degrades the system performance in terms of EE. This is due to the fact that either more power is consumed for operating the antennas or the number of antennas is not large enough for contribute to the throughput. On the other hand, in the high transmit power regime, the performance difference is smaller comparing to the one in the low transmit power regime. This is because the data rate requirement in the high transmit power regime is already satisfied because of the transmit power. Thus, the proposed scheme tends to advocate the minimum number of antennas and the performance gain due to antenna allocation becomes less significant. Moreover, it can be found that after a certain value, increment of transmit power results in the degradation of system performance, no matter what the number of antenna is used, which is similar to one observed in Fig. 6. The observations in Fig. 7 evidence the effectiveness of the antenna selection scheme and also confirms the necessity of design of antenna selection and power allocation for obtaining better EE. Moreover, it can also be found that the optimal number of selected antenna is between 10 and 50, which also show that the selection of α_s^{min} and α_s^{max} in Table 1 should have no impact on the final solution.

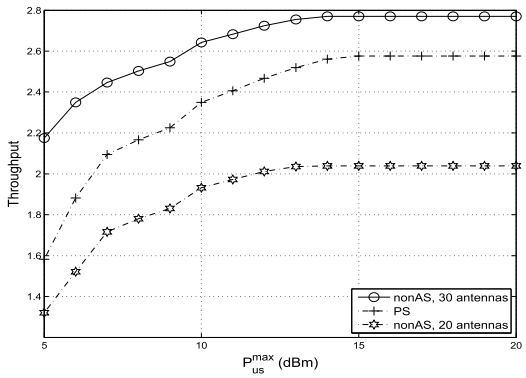

Fig. 9. Throughput vs. maximum transmit power, for different resource allocation algorithms.

Fig. 8 illustrates EE versus the maximum allowed transmit power P_{us}^{max}. It can be seen that when the maximum allowed transmit power is large enough, e.g., $P_{us}^{max} > 14\,dBm.$, the EE performance of the proposed scheme approaches a constant value since the proposed resource allocation algorithm stops consuming more power or activating more antennas, when the maximum EE is achieved. Therefore, after that, the transmit power, allocated subcarrier and number of used antennas will maintain no matter how the maximum allowed transmit power increases. For comparison, in Fig. 8, we also plot the EE performance of three resource allocation schemes. The first one, WSS scheme, is to assign different weights to different users and then allocate the resource accordingly, which is modified from [30]. The second one is that resource allocation is performed in the same manner as in the proposed scheme, except that the transmit power is equalled allocated for different users and the transmit power is set to $P_{us,n} = P_{us}^{max}/2$. The third one contains the RSS scheme together with equal power allocation. In other words, the third scheme only optimize $\boldsymbol{\omega}$ instead of $\{\boldsymbol{P}, \boldsymbol{\alpha}, \boldsymbol{\omega}\}$. Similar phenomenon can be found in these three baseline schemes except that the EE performance reach its maximum at different values of P_{us}^{max}. It can be well observed that our proposed scheme outperform the other two, which further evidences the superior performance of the presented scheme as well.

Fig. 9 shows the throughput performance in bps/Hz versus maximum transmit power. The system performance of the proposed algorithm is compared with the baseline algorithm, in which resource allocation is performed in the same manner as in the proposed one, except that the number of transmit antennas is fixed. We can see that for the PS scheme and the other two, the throughput performance approach a constant in the higher transmit power regime. This is because the proposed algorithm clips the transmit power to maximize EE. It can also be found that, as expected, the baseline scheme resource allocator with more antennas achieves a higher throughput than the PS, due to the use of more antennas. Comparing with Fig. 7, the superior throughput performance comes at the expense of low EE. On the other hand, although proposed antenna selection scheme can benefit EE of the system, there are some throughput difference comparing to the scheme that more antennas are used.

VI. Conclusion and Future Work

In this work, the energy efficient optimization for the wireless network virtualization with a large scale multiple antenna BS is studied. In particular, with the objective to obtain the energy efficiency, joint power, subcarrier, and antenna allocation problems are presented considering availability of both perfect and imperfect channel state information. Subsequently, relaxation and variable transformation are applied to develop energy efficient algorithm to solve the formulated non-convex, combinational optimization problem. Extensive simulation studies demonstrate the advantages of our presented system architecture and proposed schemes. As the future research direction, it is expected that the distributed and energy efficient resource allocation scheme can be investigated accordingly for a wireless virtualized heterogeneous networks consisting of multiple macro cells and small cells.

Appendix A: Derivation of (6)

First, for presentation simplicity, we denote $\hat{\mathbf{h}} = \hat{\mathbf{h}}_{u_s,n}$. Let $\lambda_1, \lambda_2, \lambda_3, \cdots, \lambda_N$ be the eigenvalues of $\frac{\hat{\mathbf{h}}^H\hat{\mathbf{h}}}{N}$. We also have $\rho = \rho_{u_s,n}$, then in a MIMO system with K transmit antennas and M received antennas, the mutual information is given

$$\begin{aligned} I &= \log_2 \det(\mathbf{I_K} + \frac{\rho}{K}\hat{\mathbf{h}}^H\hat{\mathbf{h}}) \\ &= \log_2 |\mathbf{I_K} + \frac{\rho M}{K}\frac{\hat{\mathbf{h}}^H\hat{\mathbf{h}}}{M}| \\ &= \log_2(1+\frac{\rho M}{K}\lambda_1)(1+\frac{\rho M}{K}\lambda_2)\cdots(1+\frac{\rho M}{K}\lambda_K) \\ &= \sum_{k=1}^{K}\log_2(1+\frac{\rho M}{K}\lambda_k), \end{aligned} \tag{33}$$

where ρ is the transmit SNR without channel gain, and $\mathbf{I_K}$ is a unit array. As for the massive MIMO UL system, $M \to \infty$, we have that $\frac{\hat{\mathbf{h}}^H\hat{\mathbf{h}}}{K} \to \mathbf{I_K}$ (strong law of large numbers, [32]). Since $\lambda_1, \lambda_2, \lambda_3, \cdots, \lambda_K$ are continuous functions of $\frac{\hat{\mathbf{h}}^H\hat{\mathbf{h}}}{M}$, it follows that $\lambda_n \to 1$ for $n = 1, 2, 3, \cdots, N$. Thus, we let $\lambda_n = 1 + \tilde{\lambda}_n$, with the understanding that $N \to \infty$, $\tilde{\lambda}_n \to 0$. Therefore, we have

$$\begin{aligned} &\sum_{k=1}^{K}\log_2(1+\frac{\rho M}{K}\lambda_k) \\ &= \log_2(1+\frac{\rho M}{K}\lambda_1)(1+\frac{\rho M}{K}\lambda_2)\cdots(1+\frac{\rho M}{K}\lambda_K) \\ &= \log_2(1+\frac{\rho M}{K})^K\frac{(1+\frac{\rho M}{K}\lambda_1)(1+\frac{\rho M}{K}\lambda_2)\cdots(1+\frac{\rho M}{K}\lambda_M)}{(1+\frac{\rho M}{K})^K} \\ &= \log_2(1+\frac{\rho M}{K})^K + \log_2(\frac{1+\frac{\rho M}{K}\lambda_1}{1+\frac{\rho M}{K}}) + \log_2(\frac{1+\frac{\rho M}{K}\lambda_2}{1+\frac{\rho M}{K}}) \\ &\quad + \cdots + \log_2(\frac{1+\frac{\rho M}{K}\lambda_K}{1+\frac{\rho M}{K}}) \\ &= M\log_2(1+\frac{\rho M}{K}) + \sum_{k=1}^{K}\log_2(\frac{1+\frac{\rho M}{K}\lambda_k}{1+\frac{\rho M}{K}}) \\ &= M\log_2(1+\frac{\rho M}{K}) + \sum_{k=1}^{K}\log_2(\frac{1+\frac{\rho M}{K}+\frac{\rho M}{K}\tilde{\lambda}_k}{1+\frac{\rho M}{K}}) \\ &= M\log_2(1+\frac{\rho M}{K}) + \sum_{k=1}^{K}\log_2(1+\frac{\frac{\rho M}{K}\tilde{\lambda}_k}{1+\frac{\rho M}{K}}) \\ &= M\log_2(1+\frac{\rho M}{K}) + \frac{\frac{\rho M}{K}log_2 e}{1+\frac{\rho M}{K}}\sum_{k=1}^{K}\tilde{\lambda}_k + O(\sum_{k=1}^{K}\tilde{\lambda}_k^2). \end{aligned} \tag{34}$$

As $M \to \infty$, we can see that $x_M = O(y_M)$ if $|x_M| \le cy_M$ for some $c > 0$ and sufficiently large M. Note that the sum of all eigenvalues $\sum_k^K \lambda_k$ is the trace of matrix $\frac{\hat{\mathbf{h}}^H\hat{\mathbf{h}}}{M}$, and

$$\begin{aligned} \sum_{k=1}^{K}\tilde{\lambda}_k &= \sum_{k=1}^{K}(\lambda_k - 1) \\ &= \lambda_1 + \lambda_2 + \cdots + \lambda_K - K = tr(\frac{\hat{\mathbf{h}}^H}{K}) - K, \end{aligned} \tag{35}$$

where $\sum_{k=1}^K \tilde{\lambda}_k$ has a zero mean. From [17, Lemma A], we can see that $E[\sum_{k=1}^K \tilde{\lambda}_k^2] = \frac{K^2}{M}$. Therefore, $O(\sum_{k=1}^K \tilde{\lambda}_k^2)$ in (34) has an expected value μ_M, which is $O(\frac{1}{M})$ as $M \to \infty$. Thus, the expected value of (34) is $K\log_2(1+\frac{\rho M}{K}) + O(\frac{1}{M})$.

By [17, Lemma A], $\sum_{k=1}^K \tilde{\lambda}_k$ has the variance $\frac{K}{M}$, and the fourth-order moment calculations of the Wishart matrix show that the variance of $\sum_{k=1}^K \tilde{\lambda}_k^2$ is $O(\frac{1}{M^2})$. Therefore, $\sum_{k=1}^K \tilde{\lambda}_k^2 - \mu_M$ is $O_p(\frac{1}{M^2})$ which is a probabilistic statement. We have that $x_M = O_p(y_M)$ if for any $\xi > 0$, we can find a certain $c > 0$ such that $P[|x_M| > cy_M] < \xi$ for a sufficiently large M [33]. From [17, Lemma B], we can also conclude that $\sqrt{\frac{M}{K}}\sum_{k=1}^K \tilde{\lambda}_k \longrightarrow \mathcal{N}(0,1)$ as $M \to \infty$. Thus, $\sum_{k=1}^K \tilde{\lambda}_k$ is $O_p(\frac{1}{M})$ and is the dominant random term in (34). The asymptotic distribution of (34) is therefore also normal [33]. Using $\frac{\frac{\rho M}{K}}{1+\frac{\rho M}{K}} = 1 + O(\frac{1}{M})$, we can see that

$$\begin{aligned} &\sum_{k=1}^{K}\log_2(1+\frac{\rho M}{K}\lambda_k) - K\log_2(1+\frac{\rho M}{K}) \\ &\quad = [1+O(\frac{1}{M})]\log_2 e\sum_{k=1}^{K}\tilde{\lambda}_k + O(\sum_{k=1}^{K}\tilde{\lambda}_k^2) \\ &\quad = \log_2 e\sum_{k=1}^{K}\tilde{\lambda}_k, \end{aligned} \tag{36}$$

which equivalents to

$$\begin{aligned} &\sqrt{\frac{M}{K}}\frac{\sum_{k=1}^K\log_2(1+\frac{\rho M}{K}\lambda_k) - K\log_2(1+\frac{\rho M}{K})}{\log_2 e} \\ &\quad = \sqrt{\frac{M}{K}}\sum_{k=1}^{K}\tilde{\lambda}_k \sim \mathcal{N}(0,1). \end{aligned} \tag{37}$$

Therefore,

$$\begin{aligned} &\sqrt{K}[\sum_{k=1}^{K}\log_2(1+\frac{\rho K}{M}\lambda_k) - K\log_2(1+\frac{\rho K}{M})] \\ &\longrightarrow \mathcal{N}(0, M\log_2^2 e), \end{aligned} \tag{38}$$

namely, $\sqrt{M}[I - K\log_2(1+\frac{\rho M}{K})] \longrightarrow \mathcal{N}(0, N\log_2^2 e)$, and correspondingly, $I \sim \mathcal{N}(M\log_2(1+\frac{\rho M}{K}), \frac{N\log_2^2 e}{M})$, and

$E[I]_{im} = N\log_2(1+\frac{\rho M}{K})$, when $N=1$, we have

$$E[I]_{im} = \log_2(1+\rho M). \tag{39}$$

APPENDIX B: PROOF OF LEMMA 1

First, for the sake of simplicity, we consider $L = \alpha_{u_s,n}$ in the following. According to [31], the mutual information when L antennas are selected for receiving can be given as

$$I = \log_2\left|1+\gamma\sum_{l=1}^{L}|h_l|^2\right|. \tag{40}$$

where γ is transmit SNR. We consider $|h_1|^2 > |h_2|^2 > ... > |h_l|^2 > ... > |h_L|^2$ and $|h_l|^2$ is chi-square random variable with two degrees of freedom. According to [34] and [35], for the order chi-square random variable with two degrees of freedom variables $z_1 > z_2 > ... > z_l > ... > z_M$, when $M \to \infty$ and $1 < L < N$ $\sum_l^L z_l$ is asymptotically normal, and $\sum_l^L z_l \sim \mathcal{N}(L(1+\ln\frac{M}{L}), L(2-\frac{L}{M}))$.

Therefore, one can observe that $\sum_l^L |h_l|^2 \sim \mathcal{N}(L(1+\ln\frac{M}{L}), L(2-\frac{L}{M}))$. Then we can reform (40) as

$$\begin{aligned} I &= \log_2\left|1+\gamma\sum_{l=1}^{L}|h_l|^2\right| \\ &= \log_2\left(1+\left(1+\ln\frac{M}{L}\right)\gamma L\right)+\log_2|z|, \end{aligned} \tag{41}$$

and z is given as

$$z = 1+\frac{\gamma\left(\sum_l^L|h_l|^2 - L(1+\ln\frac{M}{L})\right)}{1+(1+\ln\frac{M}{L})\gamma L}. \tag{42}$$

According to the distribution of $\sum_l^L|h_l|^2$, one can obtain

$$z \sim (1, \frac{\gamma^2 L(2-\frac{L}{M})}{(1+(1+\ln\frac{M}{L})\gamma L)^2}). \tag{43}$$

Given the distribution of z, the $x=|z|$ follows the folded normal distribution. With the assumption that $z \sim (\mu_z, \sigma_z^2)$ where $\mu = 1$ and $\sigma_z^2 = (\gamma^2 L(2+\frac{L}{M}))/(1+(1+\ln\frac{M}{L})\gamma L)$, the probability density function of x is

$$f(x) = \frac{1}{2\pi\sigma_z}\left(e^{\frac{x-\mu_z}{2\sigma_z^2}} + e^{\frac{x+\mu_z}{2\sigma_z^2}}\right). \tag{44}$$

It can be noticed that $\sigma_z^2 = 0$ is almost surely for large M, then I can be reformed according to Maclaurin series,

$$\begin{aligned} I &= \log_2\left(1+\left(1+\ln\frac{M}{L}\right)\gamma L\right)+log_2(1+x-1) \\ &= \log_2\left(1+\left(1+\ln\frac{M}{L}\right)\gamma L\right) \\ &\quad +(x-1)\log_2 e+\Theta((x-1)^2). \end{aligned} \tag{45}$$

$\Theta((x-1)^2)$ is very small and can be negligible so we can finally arrive at

$$\begin{aligned} I \sim \mathcal{FN}\Bigg(&\log_2\left(1+\left(1+\ln\frac{M}{\alpha_{u_s,n}}\right)\alpha_{u_s,n}\gamma\right), \\ &\frac{\gamma^2(\log_2 e)^2\alpha_{u_s,n}(2-\frac{\alpha_{u_s,n}}{M})}{\left(1+\left(1+\ln\frac{M}{\alpha_{u_s,n}}\right)\gamma\,\alpha_{u_s,n}\right)^2}\Bigg). \end{aligned} \tag{46}$$

where $\mathcal{FN}()$ is the folded normal distribution.

ACKNOWLEDGEMENT

The authors also would like to thank the editor and the anonymous reviewers for their kind comments.

REFERENCES

[1] J. G. Andrews *et al.*, "What will 5G be?" *IEEE J. Sel. Areas Commun.*, vol. 32, no. 6, pp. 1065–1082, Jun. 2014.
[2] H. Wen, P. K. Tiwary, and T. Le-Ngoc, *Wireless Virtualization*. New York, NY, USA: Springer-Verlag, 2013.
[3] C. Liang and F. R. Yu, "Wireless virtualization for next generation mobile cellular networks," *IEEE Wireless Commun.*, vol. 22, no. 1, pp. 61–69, Feb. 2015.
[4] L. Lu, G. Y. Li, A. L. Swindlehurst, A. Ashikhmin, and R. Zhang, "An overview of massive MIMO: Benefits and challenges," *IEEE J. Sel. Topics Signal Process.*, vol. 8, no. 5, pp. 742–758, Oct. 2014.
[5] C. Liang and F. R. Yu, "Wireless network virtualization: A survey, some research issues and challenges," *IEEE Commun. Surveys Tuts.*, vol. 17, no. 1, pp. 358–380, Mar. 2015.
[6] S. S. Hong, J. Mehlman, and S. Katti, "Picasso: Flexible RF and spectrum slicing," in *Proc. ACM SIGCOMM*, Helsinki, Finland, Aug. 2012, pp. 37–48.
[7] R. Kokku, R. Mahindra, H. Zhang, and S. Rangarajan, "NVS: A substrate for virtualizing wireless resources in cellular networks," *IEEE/ACM Trans. Netw.*, vol. 20, no. 5, pp. 1333–1346, Oct. 2012.
[8] M. I. Kamel, L. B. Le, and A. Girard, "LTE multi-cell dynamic resource allocation for wireless network virtualization," in *Proc. IEEE WCNC*, New Orleans, LA, USA, Mar. 2015, pp. 966–971.
[9] G. Tseliou, F. Adelantado, and C. Verikoukis, "Scalable RAN virtualization in multitenant LTE-A heterogeneous networks," *IEEE Trans. Veh. Technol.*, vol. 65, no. 8, pp. 6651–6664, Aug. 2016, doi: 10.1109/TVT.2015.2475641.
[10] J. S. Panchal, R. D. Yates, and M. M. Buddhikot, "Mobile network resource sharing options: Performance comparisons," *IEEE Trans. Wireless Commun.*, vol. 12, no. 9, pp. 4470–4482, Sep. 2013.
[11] F. Fu and U. C. Kozat, "Stochastic game for wireless network virtualization," *IEEE/ACM Trans. Netw.*, vol. 21, no. 1, pp. 84–97, Feb. 2013.
[12] Q. Zhu and X. Zhang, "Game-theory based power and spectrum virtualization for maximizing spectrum efficiency over mobile cloud-computing wireless networks," in *Proc. 49th Annu. Conf. Inf. Sci. Syst. (CISS)*, Princeton, NJ, USA, Mar. 2015, pp. 1–6.
[13] H. Zhang, W. Wang, X. Li, and H. Ji, "User association scheme in Cloud-RAN based small cell network with wireless virtualization," in *Proc. IEEE Conf. Comput. Commun. Workshops*, Hong Kong, Apr. 2015, pp. 384–389.
[14] H. Ibrahim, H. ElSawy, U. T. Nguyen, and M.-S. Alouini, "Modeling virtualized downlink cellular networks with ultra-dense small cells," in *Proc. IEEE Int. Conf. Commun. (ICC)*, London, U.K., May 2015, pp. 5360–5366.
[15] L. Chen, F. R. Yu, H. Ji, G. Liu, and V. C. M. Leung, "Distributed virtual resource allocation in small-cell networks with full-duplex self-backhauls and virtualization," *IEEE Trans. Veh. Technol.*, vol. 65, no. 7, pp. 5410–5423, Jul. 2016.
[16] E. G. Larsson, O. Edfors, F. Tufvesson, and T. L. Marzetta, "Massive MIMO for next generation wireless systems," *IEEE Commun. Mag.*, vol. 52, no. 2, pp. 186–195, Feb. 2014.
[17] B. M. Hochwald, T. L. Marzetta, and V. Tarokh, "Multiple-antenna channel hardening and its implications for rate feedback and scheduling," *IEEE Trans. Inf. Theory*, vol. 50, no. 9, pp. 1893–1909, Sep. 2004.
[18] T. Gucluoglu and E. Panayirci, "Performance of transmit and receive antenna selection in the presence of channel estimation errors," *IEEE Commun. Lett.*, vol. 12, no. 5, pp. 371–373, May 2008.
[19] H. Li, L. Song, and M. Debbah, "Energy efficiency of large-scale multiple antenna systems with transmit antenna selection," *IEEE Trans. Commun.*, vol. 62, no. 2, pp. 638–647, Feb. 2014.
[20] V. Jumba, S. Parsaeefard, M. Derakhshani, and T. Le-Ngoc, "Resource provisioning in wireless virtualized networks via massive-MIMO," *IEEE Wireless Commun. Lett.*, vol. 4, no. 3, pp. 237–240, Jun. 2015.
[21] Z. Chang, T. Ristaniemi, and Z. Niu, "Radio resource allocation for collaborative OFDMA relay networks with imperfect channel state information," *IEEE Trans. Wireless Commun.*, vol. 13, no. 5, pp. 2824–2835, May 2014.

[22] W. Dinkelbach, "On nonlinear fractional programming," *Manage. Sci.*, vol. 13, no. 7, pp. 492–498, Mar. 1967.
[23] W. Yu and R. Lui, "Dual methods for nonconvex spectrum optimization of multicarrier systems," *IEEE Trans. Commun.*, vol. 54, no. 7, pp. 1310–1322, Jul. 2006.
[24] W. Dang, M. Tao, H. Mu, and J. Huang, "Subcarrier-pair based resource allocation for cooperative multi-relay OFDM systems," *IEEE Trans. Wireless Commun.*, vol. 9, no. 5, pp. 1640–1649, May 2010.
[25] S. Boyd and A. Mutapcic, *Lecture Notes for EE364b*. Stanford, CA, USA: Stanford Univ., pp. 2006–2007.
[26] D. W. K. Ng, E. S. Lo, and R. Schober, "Energy-efficient resource allocation in OFDMA systems with large numbers of base station antennas," *IEEE Trans. Wireless Commun.*, vol. 11, no. 9, pp. 3292–3304, Sep. 2012.
[27] J. Joung, Y. K. Chia, and S. Sun, "Energy-efficient, large-scale distributed-antenna system (L-DAS) for multiple users," *IEEE J. Sel. Topics Signal Process.*, vol. 8, no. 5, pp. 954–965, Oct. 2014.
[28] S. Cui, A. J. Goldsmith, and A. Bahai, "Energy-efficiency of MIMO and cooperative MIMO techniques in sensor networks," *IEEE J. Sel. Areas Commun.*, vol. 22, no. 6, pp. 1089–1098, Aug. 2004.
[29] Á. R. C. e Souza, J. R. de Almeida Amazonas, and T. Abrão, "Power and subcarrier allocation strategies for energy-efficient uplink OFDMA systems," *IEEE J. Sel. Areas Commun.*, vol. 34, no. 12, pp. 3142–3156, Dec. 2016, doi: 10.1109/JSAC.2016.2600409.
[30] L. Xu, G. Yu, and Y. Jiang, "Energy-efficient resource allocation in single-cell OFDMA systems: Multi-objective approach," *IEEE Trans. Wireless Commun.*, vol. 14, no. 10, pp. 5848–5858, Oct. 2015.
[31] E. Telatar, "Capacity of multi-antenna Gaussian channels," *Trans. Emerg. Telecommun. Technol.*, vol. 10, pp. 585–595, Nov/Dec. 1999.
[32] P. Billingsley, *Probability and Measure*, 2nd ed. New York, NY, USA: Wiley, 1986.
[33] Y. S. Chow and H. Teicher, *Probability Theory: Independence, Interchangeability, Martingales*. New York, NY, USA: Springer-Verlag, 1988.
[34] S. M. Stigler, "The asymptotic distribution of the trimmed mean," *Ann. Statist.*, vol. 1, no. 3, pp. 472–477, May 1973.
[35] P. Hesami and J. N. Laneman, "Limiting behavior of receive antennae selection," in *Proc. Annu. CISS*, Baltimore, MD, USA, Mar. 2011, pp. 1–6.

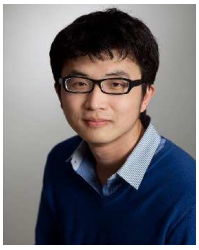

Zheng Chang (M'13) received the B.Eng. degree from Jilin University, Changchun, China, in 2007, the M.Sc. (Tech.) degree from Aalto University, Espoo, Finland, in 2009, and the Ph.D. degree from the University of Jyväskylä, Jyväskylä, Finland, in 2013. Since 2008, he has held various research positions with Aalto University, the University of Jyväskylä, and Magister Solutions Ltd., Finland. He was a Visiting Researcher with Tsinghua University, China, in 2013, and the University of Houston, TX, in 2015. He is currently with the University of Jyväskylä. His research interests include radio resource allocation, Internet of Things, cloud computing, and green communications. He has been awarded by the Ulla Tuominen Foundation, the Nokia Foundation, and the Riitta and Jorma J. Takanen Foundation for his research work.

Zhu Han (S'01–M'04–SM'09–F'14) received the B.S. degree in electronic engineering from Tsinghua University, in 1997, and the M.S. and Ph.D. degrees in electrical and computer engineering from the University of Maryland, College Park, in 1999 and 2003, respectively.

From 2000 to 2002, he was a Research and Development Engineer with JDSU, Germantown, MD. From 2003 to 2006, he was a Research Associate with the University of Maryland. From 2006 to 2008, he was an Assistant Professor with Boise State University, Idaho. He is currently a Professor with the Electrical and Computer Engineering Department and the Computer Science Department, University of Houston, TX. His research interests include wireless resource allocation and management, wireless communications and networking, game theory, big data analysis, security, and smart grid. He received the NSF Career Award in 2010, the Fred W. Ellersick Prize of the IEEE Communication Society in 2011, the EURASIP Best Paper Award for the *Journal on Advances in Signal Processing* in 2015, the IEEE Leonard G. Abraham Prize in the field of Communications Systems (Best Paper Award in the IEEE JOURNAL ON SELECTED AREAS IN COMMUNICATIONS) in 2016, and several best paper awards in the IEEE conferences. He is also the IEEE Communications Society Distinguished Lecturer.

Tapani Ristaniemi (SM'11) received the M.Sc. degree in mathematics, the Ph.Lic. degree in applied mathematics, and the Ph.D. degree in wireless communications from the University of Jyväskylä, Jyväskylä, Finland, in 1995, 1997, and 2000, respectively. In 2001, he was appointed as a Professor with the Department of Mathematical Information Technology, University of Jyväskylä. In 2004, he moved to the Department of Communications Engineering, Tampere University of Technology, Tampere, Finland, where he was appointed as a Professor in Wireless Communications. In 2006, he moved back to the University of Jyväskylä to take up his appointment as a Professor in Computer Science. In 2013, he was a Visiting Professor with the School of Electrical and Electronic Engineering, Nanyang Technological University, Singapore. He is currently an Adjunct Professor with the Tampere University of Technology.

He has authored or co-authored over 150 publications in journals, conference proceedings, and invited sessions. His research interests are in the areas of brain and communication signal processing and wireless communication systems research. He served as a Guest Editor of the IEEE WIRELESS COMMUNICATIONS in 2011. He is currently an Editorial Board Member of *Wireless Networks* and the *International Journal of Communication Systems*.

Besides academic activities, he is also active in industry. In 2005, he co-founded a start-up Magister Solutions Ltd., Finland, which specializes in wireless system research and development for telecom and space industries in Europe. He currently serves as a Consultant and a member of the Board of Directors.